Influence of Torch Nozzle Geometry on Plasma Jet Properties

O. Chang, A. Kaminska, M. Dudeck

Influence of Torch Nozzle Geometry on Plasma Jet Properties

O.H. Chang ([1]), A. Kaminska ([2]) and M. Dudeck ([2,*])

([1]) Institute of Electric Power Engineering, Poznan University of Technology, ul. Piotrowo 3A, 60-965 Poznan, Poland

([2]) Laboratoire d'Aérothermique du CNRS, 92190 Meudon, 4ter, route des Gardes, France

(Received 29 July 1996, revised 4 February 1997, accepted 26 February 1997)

PACS.52.50.Dg – Plasma sources

PACS.52.75.Hn – Plasma torches

Abstract. — The influence of torch nozzle geometry on plasma jet properties is investigated using a non-equilibrium model. A code is developed to numerically solve the conservation equations of mass, momentum and energies by means of finite difference method. The distributions of pressure, temperatures, electron density and velocities are studied for different angles and lengths of plasma torch nozzle and the possibility of generating a wide variety of plasma jets by changing the geometry of the plasma torch nozzle is demonstrated.

Résumé. — L'influence de la géométrie de la tuyère d'une source de plasma à arc est étudiée en utilisant un modèle hors-équilibre. Un code numérique a été développé pour résoudre numériquement les équations de conservation de masse, de quantité de mouvement et d'énergies à partir d'une méthode de différences finies. Les distributions de pression, températures, densité électronique et vitesses ont été étudiées pour différents angles et longueurs de la tuyère et la possibilité de créer une grande variété de jets de plasma en changeant la géométrie de la tuyère est démontrée.

1. Introduction

The thermal plasma jets are widely used for industrial applications and in the laboratories for simulation of physical phenomena. For these aims, plasma jets of different properties such as temperature, velocity, pressure and composition, are necessary. The thermal plasma jets have temperature below 25 000 K, subsonic or supersonic velocities and the range of pressures 100 kPa – 1 Pa. A wide variety of plasma torches is used to obtain plasma jets. The construction of torch nozzle has a crucial importance in the production of different regimes of plasma flow. The cylindrical nozzles are, most often used, to produce the subsonic plasma jets, in equilibrium conditions (except near the wall) with high temperature and near the atmospheric pressure. The divergent nozzles allow to produce supersonic non-equilibrium jets with lower temperatures and pressures. For applications, a good knowledge and control of the plasma is very important. Therefore, it is essential to have a model allowing to simulate different plasma

(*) Author for correspondence (e-mail: dudeck@cnrs-bellevue fr).

jets. This model has to take into account correctly phenomena occurring in wide variety of plasma jet conditions: high speed flow, deviations from thermal and chemical equilibrium, diffusion and heat conduction. Over the past years, extensive experimental and theoretical works on plasma torches have been conducted. However, most of the investigations were valid to atmospheric pressure plasma jets in cylindrical nozzles, which justifies the assumption of LTE. In divergent nozzles a strong expansion of plasma is obtained [1,3,4] and modelling work for atmospheric pressure plasma jet may not be applicable to the expanding plasma jets. In a realistic analysis of low-pressure, high-speed plasma jets deviations from LTE must be taken into account [5,6].

The plasma jets are described by the conservation equations of mass, momentum and energy, with state equation and Dalton's law. These equations are solved using finite difference method or finite volume method. Among these methods, Patankar-Spalding's [7] is the most popular, this method is applied to solve non-equilibrium plasma equations [5, 8], equilibrium plasma system [9] and the boundary layer equations.

In this paper, the possibility of producing a wide variety of plasma jets, by changing the geometry of the nozzle, is shown. By this way, it is possible to obtain subsonic and supersonic, low and atmospheric pressure plasma jets in equilibrium and non-equilibrium conditions. Therefore, it is necessary to elaborate a model taking into account these situations. In the model, the plasma is treated as a two-component and two-temperature mixture that contains heavy species (neutral atoms and ions) and electrons. For description of these plasmas the continuity, momentum and energy equations for heavy species and electrons are solved by finite difference method.

The calculations are performed with argon for cylindrical and divergent nozzles. For different geometrical conditions, the temperatures, velocities, pressure and plasma composition were investigated.

2. Plasma Torches

The modelling is applied in the case of plasma torches used at Laboratoire d'Aérothermique (Fig. 1a) and Institute of Electric Power Engineering (Fig. 1b). The plasma jets are produced by a torch with a stationary regime.

At the Laboratoire d'Aérothermique, the cathode, made of thoriated tungsten ($W+3\%ThO_2$) or zirconium is placed in a water-cooled support. The anode, made of cooper consists of a cylindrical part and a divergent part. The electrical insulation between the two parts is obtained using an insulating part in which holes were drilled to inject the gas.

At the Institute of Electric Power Engineering, a plasma torch with cylindrical segmented nozzle is used, the diameter is 12 mm and its length 30 mm. The cathode is a 8 mm long and 6 mm in diameter thoriated tungsten ($W+3\%ThO_2$) rod, mounted on a water-cooled support. The plasma torch chamber is formed by 6 segments insulated from each other by disc with the gas injection channels. The electric arc between cathode and the first segment produces a plasma jet which develops along the chamber of torch.

3. Modelling

3.1. Governing Equations. — For modelling of plasma jets produced by the electric arc, several assumptions are taken into account: the electric arc is formed in the cylindrical part of the torch and the plasma jet in the divergent or cylindrical part, stationary processes are considered, the argon plasma is assumed to be single ionized, locally quasi-neutral, with local

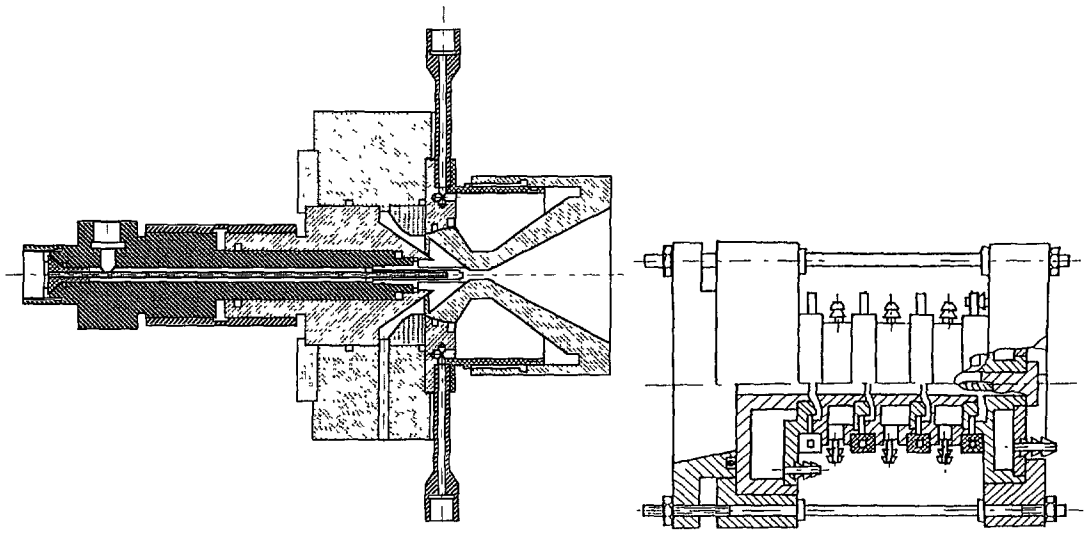

a) b)

Fig. 1. — Plasma torches: a) used at the Laboratoire d'Aérothermique, b) used at the Institute of Electric Power Engineering.

temperature non-equilibrium, the electrical field is supposed to be one-dimensional and uniform over the arc cross section.

The complete description of the non-equilibrium plasma flow is given by the degree of ionization, velocities, electron and heavy species temperatures and pressure. These variables are determined by solving the continuity, momentum, composition and energies equations. Using cylindrical co-ordinates, and considering the above-mentioned assumptions, we can write the governing equations as follows. As first approximation, the continuity and momentum equations for axisymmetric, supersonic, laminar jets are written as:

$$\frac{\partial}{\partial z}(\rho u) + \frac{1}{r}\frac{\partial}{\partial r}(r\rho v) = 0 \tag{1}$$

$$\rho u\frac{\partial u}{\partial z} + \rho v\frac{\partial u}{\partial r} = \frac{1}{r}\frac{\partial}{\partial r}\left(r\mu\frac{\partial u}{\partial r}\right) - \frac{\partial p}{\partial z} \tag{2}$$

$$\rho u\frac{\partial v}{\partial z} + \rho v\frac{\partial v}{\partial r} = \frac{2}{r}\frac{\partial}{\partial r}\left(r\mu\frac{\partial v}{\partial r}\right) - \frac{2\mu v}{r^2} - \frac{\partial p}{\partial r} \tag{3}$$

where u and v are the axial and radial velocities, ρ is the plasma mass density, p is the pressure and μ is the viscosity, z and r are the axial and radial co-ordinates.

The plasma density is calculated by neglecting electron density: $\rho = (n_i + n_n)m_h$ and the plasma pressure by Dalton's law: $p = (n_i + n_n)kT + n_e kT_e$ where n_n, n_e and n_i are the number densities of neutral atoms, electrons and ions respectively, m_h is the heavy species mass, k is the Boltzmann constant, T and T_e are heavy species and electron temperatures respectively. With the local quasi neutrality assumption $n_i \approx n_e$, and introducing the heavy species number density $n_h = n_i + n_n$ the equation of state becomes: $p = n_k k(T + \alpha T_e)$ where $\alpha = n_e/n_h$ denotes the ionization degree.

For a single ionized, monatomic gas, at locally quasi neutral conditions the diffusion process is controlled by ambipolar diffusion and the electron conservation equation is:

$$\frac{\partial}{\partial z}(n_e u) + \frac{1}{r}\frac{\partial}{\partial r}(r n_e v) = \frac{1}{r}\frac{\partial}{\partial r}\left(rD\frac{\partial n_e}{\partial r}\right) + \dot{w}_e \tag{4}$$

where D is the ambipolar diffusion coefficient and $\dot{w}_e$ is the electron source term.
Substituting the electron density n_e for the degree of ionization α, and taking into account the continuity equation (1) we obtain:

$$\rho u\frac{\partial \alpha}{\partial z} + \rho v\frac{\partial \alpha}{\partial r} = \frac{1}{r}\frac{\partial}{\partial r}\left(r\rho D\frac{\partial \alpha}{\partial r}\right) + m_h \dot{w}_e. \tag{5}$$

There are three possible mechanisms of recombination: electron-electron-atom three-body collisions, electron-atom-atom three-body collisions and radiative processes. In typical low-pressure plasma jets, the electron density is around 10^{20} m^{-3} and the first process is the most important. Therefore, as a first approximation, we consider three-body recombination, with an electron as the third body, as the predominant recombination process and electron atom collision as the predominant ionization process, consequently the following chemical reaction is taken into account: $Ar + e^- \leftrightarrow Ar^+ + e^- + e^-$. However, because of the high velocities, deviation from ionization equilibrium will be further enhanced. In extreme cases a "frozen flow", the chemical reactions (ionization and recombination) cannot follow the fast macroscopic translation of charged particles in the plasma jet. This deviation from chemical or ionization equilibrium will manifest itself by substantially higher electron densities than one would expect from the prevailing temperatures. For the following analysis, the model of Hoffert-Lien [10] will be adopted because the good agreement with experiments. The electron source term is:

$$\dot{w}_e = \frac{dn_e}{dt} = k_{ion} n_n n_e - k_{re} n_e^3.$$

The ionization rate coefficient k_{ion} can be expressed as follows [10]:

$$k_{ion} = 8S_1(2\pi m_e)^{-1/2}(kT_e)^{3/2}\left(\frac{E_{1*}}{2kT_e} + 1\right)\exp\left(-\frac{E_{1*}}{kT_e}\right)$$

where E_{1*} is the first excitation energy and S_1 is the cross-section parameter which is a constant for a given atom. For argon, the values of S_1 and E_{1*} are 7.0×10^{-18} cm^2 eV^{-1} and 11.67 eV respectively [10].
The recombination rate can be calculated from the equilibrium relation:

$$K_{eq} = \frac{k_{ion}}{k_{re}} \quad \text{and} \quad K_{eq} = \frac{2Z_i^e}{Z_n^e}\left(\frac{2\pi m_e kT_e}{h^2}\right)^{3/2}\exp\left(-\frac{E_{ion}}{kT_e}\right)$$

where h is Planck's constant. The ionization energy is defined by $E_{ion} = e(E_0 - \Delta E)$, where $E_0 = 15.76$ eV and the lowering of the ionization energy due to electric ions field is given by $\Delta E = 2.086 \times 10^{-11}\sqrt{2n_e/T_e}$ in eV. The electronic partition functions of Ar^+ and Ar according to Drawin and Felenbok [11] are:

$$Z_n^e = 1 \quad \text{and} \quad Z_i^e = 4 + 2\exp(-2059/T_e)$$

The energy equation for heavy particles is transformed into

$$\frac{5}{2}kn_h\left(u\frac{\partial T}{\partial z} + v\frac{\partial T}{\partial r}\right) = \frac{1}{r}\frac{\partial}{\partial r}\left(r\kappa\frac{\partial T}{\partial r}\right) + u\frac{\partial}{\partial z}(kTn_h) + v\frac{\partial}{\partial r}(kTn_h) + B(T_e - T) \tag{6}$$

and the electron energy equation is

$$\frac{5}{2}kn_e\left(u\frac{\partial T}{\partial z}+v\frac{\partial T_e}{\partial r}\right)=\frac{1}{r}\frac{\partial}{\partial r}\left(r\kappa_e\frac{\partial T_e}{\partial r}\right)+u\frac{\partial}{\partial z}(n_ekT_e)+v\frac{\partial}{\partial r}(n_ekT_e)-E_{ion}\dot{w}_e+\Psi-B(T_e-T) \tag{7}$$

where κ and κ_e are respectively heavy particle and electron heat conductivities.
The source term $B(T_e-T)$ is the energy exchange between electrons and heavy species due to elastic collisions with the coefficient B represented by

$$B=3kn_e\frac{m_e}{m_h}\nu_{eh}$$

where $\nu_{eh}=\nu_{ei}+\nu_{en}$ are the average elastic collision frequencies between electron-ion (ν_{ei}) and electron-neutral (ν_{en}):

$$\nu_{ei}=\frac{e^4n_e\ln\Lambda}{12\pi\varepsilon_0^2\sqrt{2\pi m_ek^3T_e^3}},\quad \nu_{en}=n_n\langle Q_{en}\rangle\sqrt{\frac{8kT_e}{\pi m_e}}.$$

The Coulomb logarithm $\ln\Lambda$ is given by:

$$\ln\Lambda=\ln\left(6\sqrt{2\pi}\left(\frac{\varepsilon_0k}{e^2}\right)^{3/2}\sqrt{\frac{T_e^3}{n_e}}\right)$$

where e is the electron charge, ε_0 is the permeability.
This value is lower than the value obtained from a definition of the Debye length without taking into account the shielding of the ions. The value of Coulomb logarithm may have an important influence on the results of temperature calculation for high-density low-temperature plasmas. In our case this influence is not important.
The average electron-neutral collision cross section is calculated by the semi-empirical expression [8]:

$$\langle Q_{en}\rangle=2.8\times10^{-24}T_e-4.1\times10^{-34}T_e^3-3\times10^{-21}\quad\text{in}\quad(\text{m}^2).$$

The radiative term in strongly flowing plasma jets is small compared to the convective term. However, the calculations are performed taken into account electron-neutral free-free radiation Q_{rad}^{e-o}, electron-ion free-free radiation Q_{rad}^{e-i}, and the line radiation Q_{rad}^{line} [8]:

$$\Psi=Q_{rad}^{e-o}+Q_{rad}^{e-i}+Q_{rad}^{line}$$

where $Q_{rad}^{e-0}=53.759\bar{n}_e^{1.25}\bar{n}_0$, $Q_{rad}^{e-i}=910\,\bar{n}_e^2$, $Q_{rad}^{line}=2.572\times10^4\,\bar{n}_e^{1.57}$ and the dimensionless electron density is determined as $\bar{n}_e=n_e/10^{20}$ and the dimensionless neutral density is $\bar{n}_0=n_0/10^{24}$.

3.2. Physical Properties of Plasma. — The numerical solving of plasma conservation equations requires the calculation of transport coefficients. These coefficients are function of four variables: electron and heavy species densities and electron and heavy species temperatures.

The thermal conductivity is calculated as a sum of three components: the thermal conductivity due to the particle translational energy, the thermal conductivity attached to the internal energies and the thermal conductivity due to the chemical reactions. The translational thermal conductivity coefficient is calculated using the first approximation of the Chapmann-Enskog method [12]. The reactive term contribution is determined using the theory of Butler and

Brokav [13] as extended to the case of partially ionized gases and internal thermal conductivity is calculated by Eucken method [14].

The electronic thermal conductivity is determined by the following equation [15]:

$$\kappa_e = \frac{90}{8}\frac{10^{28}}{m_e}\frac{1}{1.349\ln\Lambda}k^3T^{5/2}.$$

The plasma viscosity is calculated from the definition of the Prandtl number, with the assumption of $P_r = 2/3$, $\mu = \Pr(\lambda/c_p)$, where the specific heat coefficient c_p, at constant pressure is evaluated by numerical differentiation of the total enthalpy which is the sum of the enthalpies of atoms, ions and electrons

The ambipolar diffusion coefficient is determined by the expression of Devoto [16], $D = 3kT_e/4\rho\Omega_{in}$, in which Ω_{in} is the first approximation to the ion-atom collision integral [8] $\Omega_{in} = 2.84 \times 10^{-17}T^{0\,36}$ in $(m^3\,s^{-1})$.

3.3. Boundary Conditions. — The system of partial differential plasma flow equations is solved with the boundary conditions specified for the inlet of divergent part of the nozzle, axis and wall.

• At the inlet of divergent part, the boundary conditions are specified by arc plasma model [17] allowing to determine temperature and velocity distributions for different operating parameters of plasma torch such as arc current, gas flow rate and pressure. Temperature equilibrium and non-equilibrium conditions are studied.

• On the axis, axisymmetric conditions are satisfied:

$$\frac{\partial T_e}{\partial r} = \frac{\partial T}{\partial r} = 0, \quad \frac{\partial \alpha}{\partial r} = 0, \quad \frac{\partial u}{\partial r} = 0, \quad v(0,z) = 0.$$

• On the wall, adiabatic and isothermal conditions are tested. For isothermal conditions, the arbitrary values $T_{wall} = 1000$ K and $T_{e,\,wall} = 6000$ K are chosen with no-slip conditions on velocities.

3.4. Numerical Method. — The previous equations (1–7) of continuity, momentum, composition and energies for electrons and heavy species have the general form:

$$a_m\frac{\partial F_m}{\partial r} + b_m\frac{\partial F_m}{\partial z} = \frac{\partial}{\partial r}\left(c_m\frac{\partial F_m}{\partial r}\right) + d_m.$$

A finite difference method is used, the discretization of the nonlinear 2nd order differential equation being obtained according to the differential diagram of two layers i, $i+1$, and six points k, $k-1$, $k+1$ [18]. On the wall, for the pressure and densities, the zero-gradient extrapolation is applied. The pressure and velocity correction equations are solved by numerical method of Patankar and Spalding [7].

Taking into account the conical geometry of the divergent and axisymmetry of the problem, the following numerical grid is considered (Fig. 2):

$$\xi_{\Delta z,\,\Delta r} = \xi\{r_{i,\,k} = (k-1)\Delta r_i,\ k = 1,\ \ldots,\ Nr,\ r_{i,\,1} = 0,\ r_{i,\,Nr} = r_c;$$
$$z_i,\ i = 1\ldots,\ Nz,\ z_1 = 0,\ z_{Nz} = z_{max}\}$$

where a finer grid generation is used for z_i [19]:

$$z_i = \left[ps + (1-p)\frac{[1-\tanh(q(1-s))]}{\tanh(q)}\right](z_{Nz} - z_1),$$

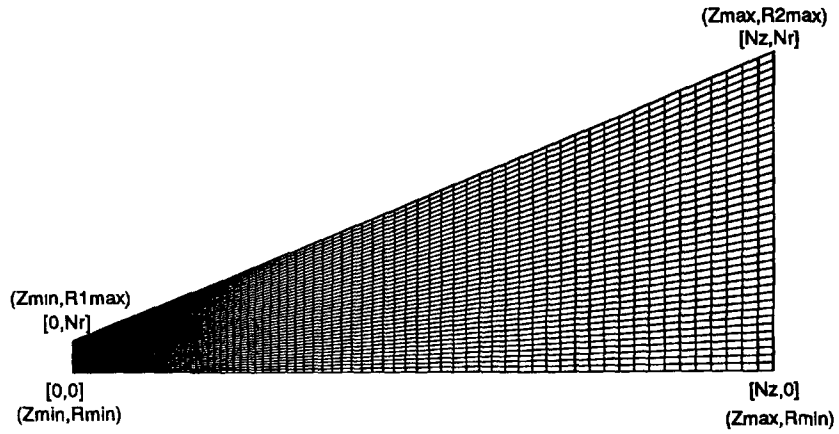

Fig 2. — Computational grid.

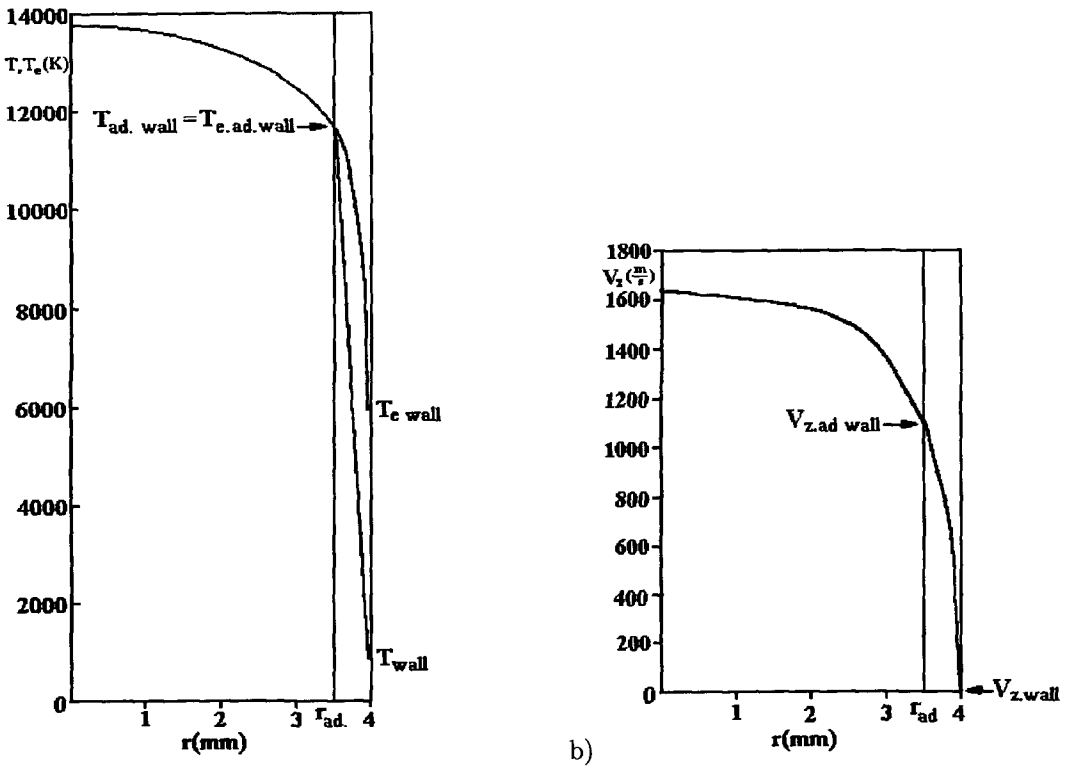

Fig. 3. — Inflow boundary conditions with real and adiabatic wall, a) electron and heavy particle temperature, b) axial velocity.

with $s = \dfrac{i-1}{Nz-1}$, $p = 0.1$, $q = 2.0$ and Δr_i determined as

$$\Delta r_i = r_{i,\,k+1} - r_{i,\,k} = \frac{\frac{R_{\max}-R_{\min}}{z_{\max}} z_i + R_{\min}}{Nr-1}.$$

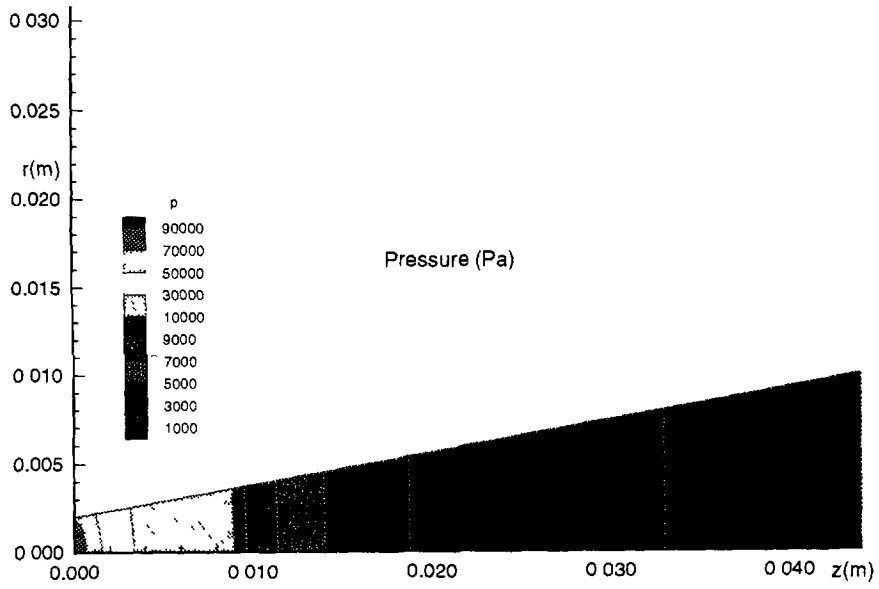

Fig. 4. — Pressure field in the divergent nozzle of exit diameter 20 mm.

An auxiliary grid is also introduced for the calculation of different discretized terms:

$$\xi_{\Delta r/2,\ \Delta z/2} = \xi\{r_{i,\ k\pm 1/2} = (k \pm 1/2)\Delta r_i,\ z_{i+1/2} = (i + 1/2)\Delta z_i\}.$$

The numerical solution is assumed to be converged when the following condition is verified:

$$\left| 1 - \frac{(F_m^{i+1,\ k})_n}{(F_m^{i+1,\ k})_{n-1}} \right| \leq 0.01.$$

The previous numerical method is used to elaborate the simulation program of plasma jet. This program allows to analyse the flow for different shapes of nozzle with the angle of divergence varying from 0° (cylindrical nozzle) to 80° and for different operating parameters of plasma torch.

4. Results

The calculations are performed for cylindrical and divergent nozzles. The diameter of the cylinder is 4 mm. Two shapes of divergent nozzle are studied: inlet diameter of divergent is the same 4 mm, while the exit diameters are different: 20 mm and 40 mm. We have also compared the results for two different lengths of the nozzle· 44 mm and 88 mm. The calculations are carried out for the inlet pressure of 95 kPa, the mass flow rate of 0.5 g s^{-1} and arc current of 400 A. For these different geometrical conditions and the constant operating plasma torch conditions, the temperatures, velocities, pressure and plasma composition are investigated.

The inflow boundary conditions are specified at the beginning of the divergent part of the nozzle. At first, the calculations are performed for the entry temperature and velocity distributions shown in Figure 3 and for the real wall with no-slip conditions on velocities, $T_{\text{wall}} = 1000$ K

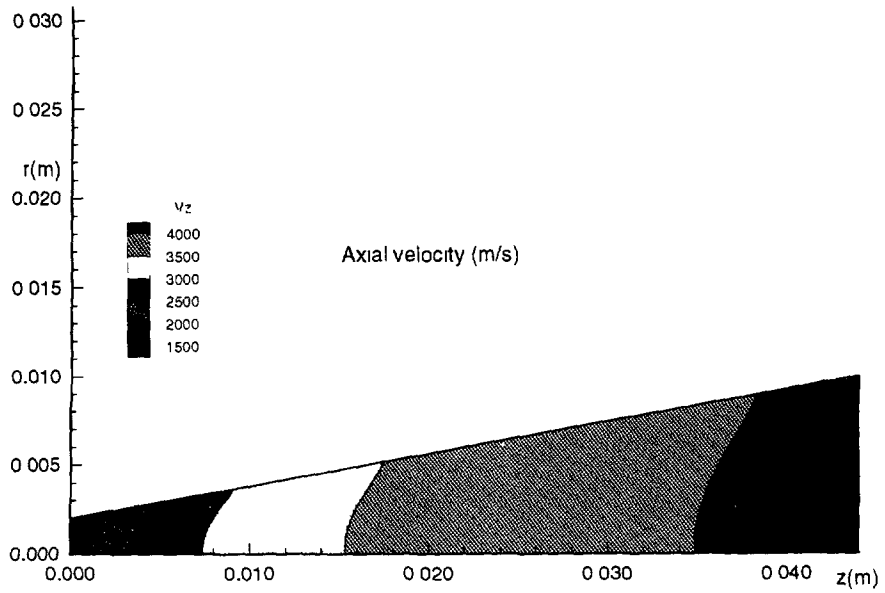

Fig. 5 — Axial velocity field in the divergent nozzle of exit diameter 20 mm.

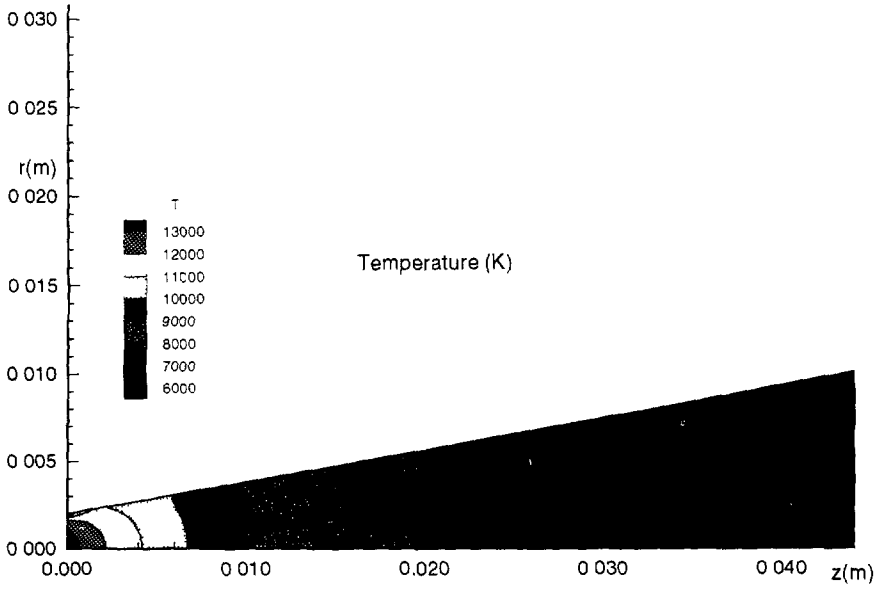

Fig. 6. — Heavy particle temperature field in the divergent nozzle of exit diameter 20 mm.

and $T_{e,\,wall} = 6000$ K. Because of strong gradients near the wall, a fine grid is used and the calculation becomes very time consuming. Therefore, we use imaginary wall with adiabatic and slip conditions (Fig. 3). The calculating test for both wall conditions proves little influence on the results in the central part of the nozzle except in thin layer near the wall. It's the reason why we used the numerical model with assumption of adiabatic wall.

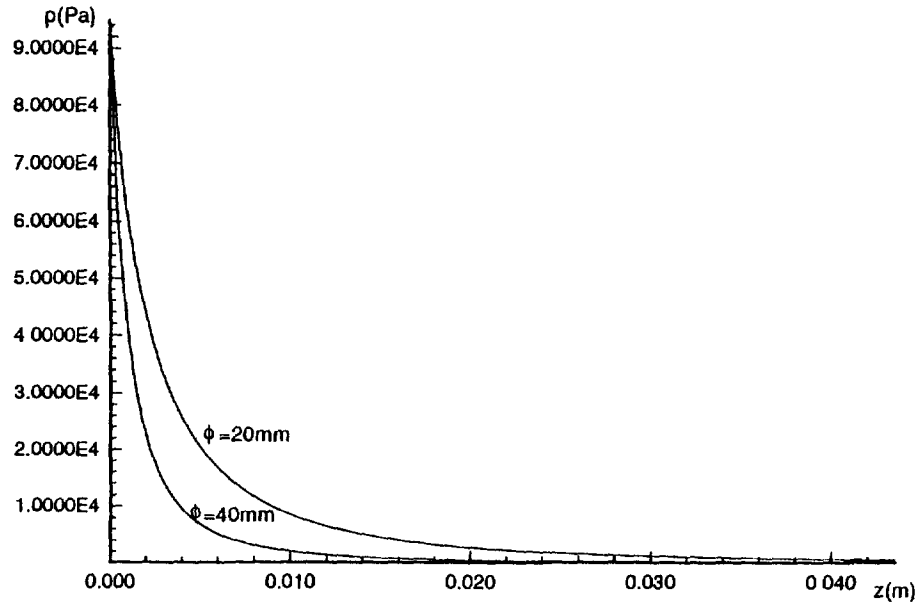

Fig. 7. — Axial distributions of pressure for different shapes of nozzle.

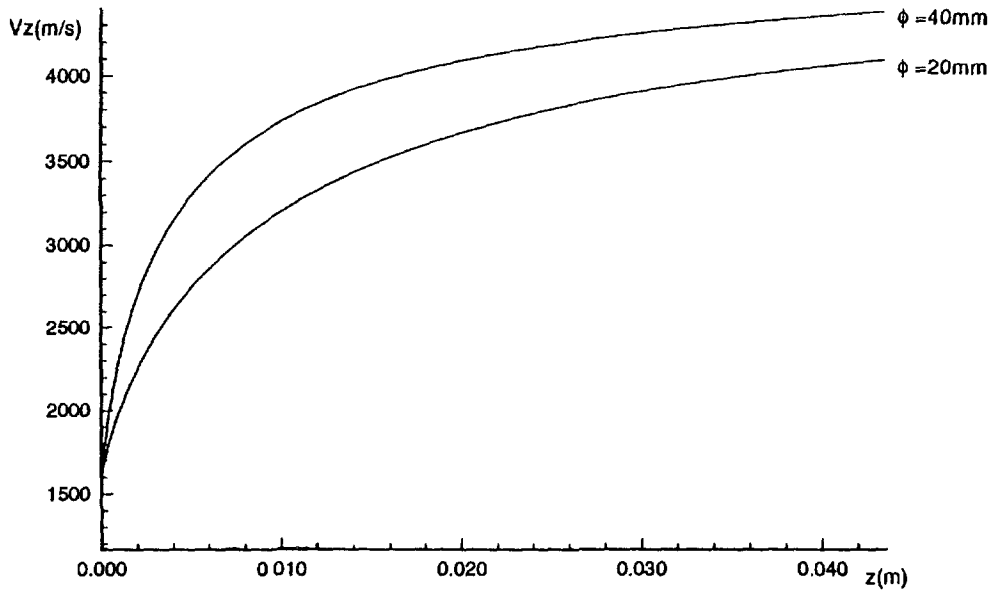

Fig. 8. — Axial distributions of velocity for different shapes of nozzle.

The pressure, velocity and temperature in the cylindrical nozzle (with mass flow rate 0.5 g s^{-1} and arc current 400 A), vary very slightly compared to the divergent nozzle case: the pressure decreases along the axis from 95 kPa to 83 kPa, consequently a small increase of the axial velocity (from 1630 to 1740 m s^{-1}) is observed due to the weak value of the term $\partial p/\partial z$ in the

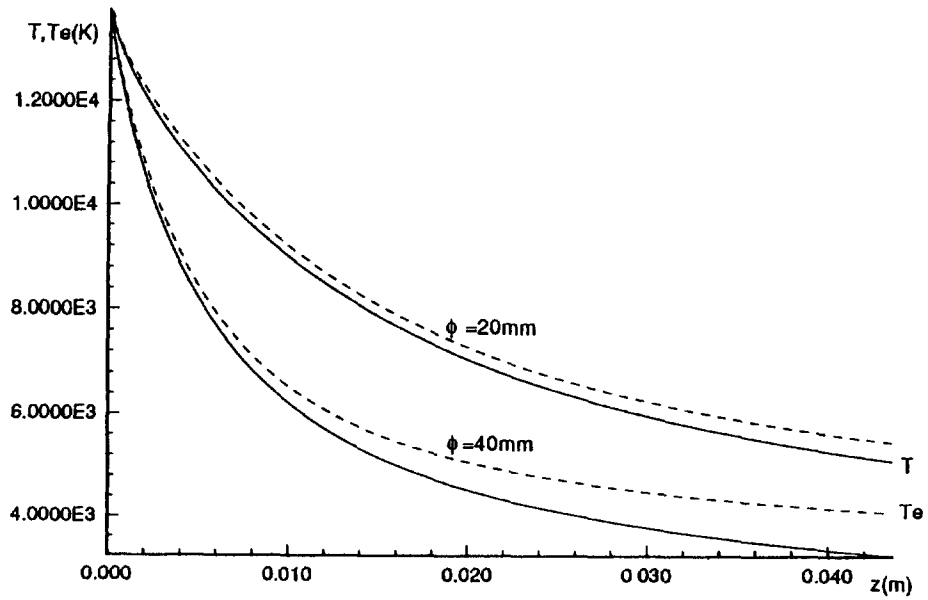

Fig. 9. — Axial distributions of heavy particle and electron temperatures for different shapes of nozzle.

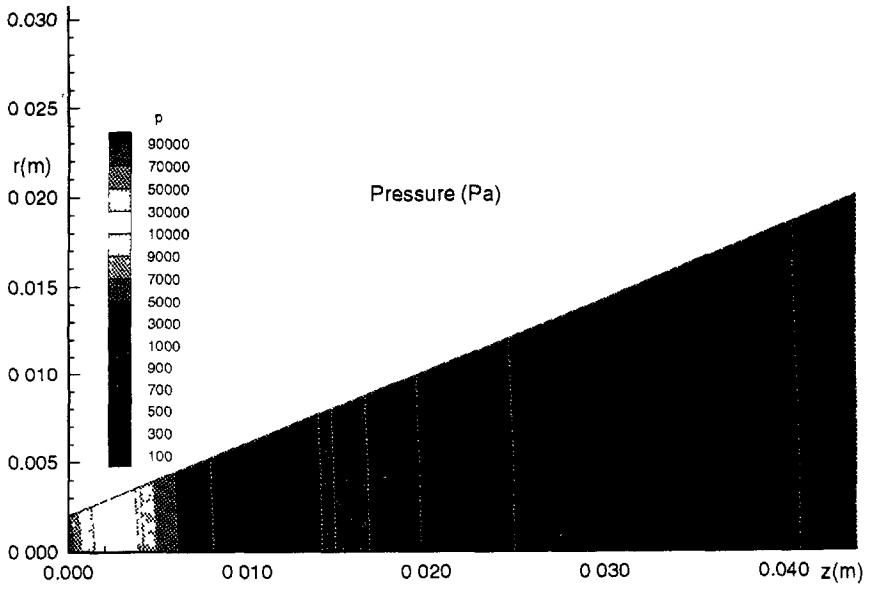

Fig 10. — Pressure field in the divergent nozzle of exit diameter 40 mm.

momentum conservation equation, the temperatures remain high (from 13 700 K at the inlet to 12 900 K at the exit) and in equilibrium during all the evolution. An important influence of the wall conditions on the temperature distribution, due to the radial conductive heat flux, is observed.

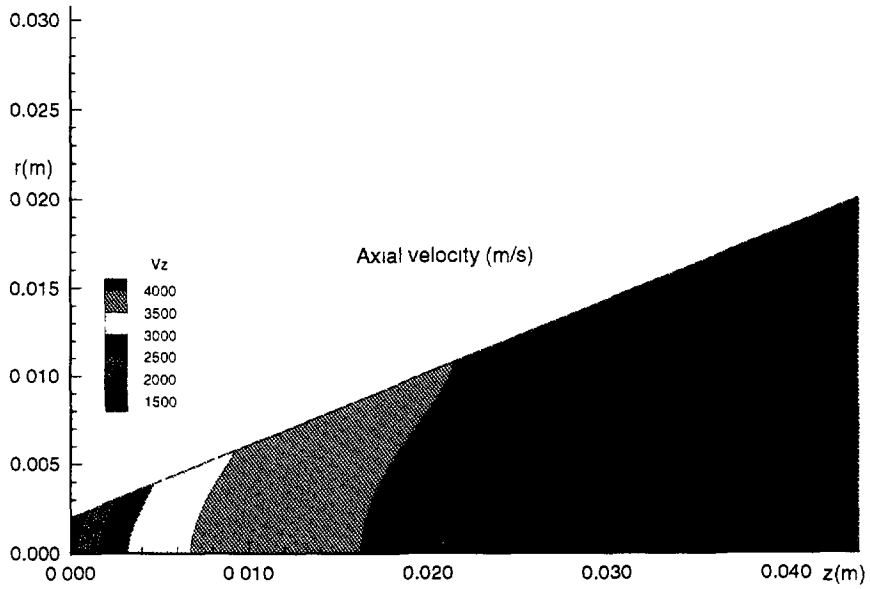

Fig. 11. — Axial velocity field in the divergent nozzle of exit diameter 40 mm.

The fields of the pressure (Fig. 4), axial velocity (Fig. 5) and heavy species temperature (Fig. 6) in the divergent nozzle of exit diameter 20 mm are shown. The expansion of the plasma jet causes sudden decrease of the pressure, from 95 kPa to 539 Pa (Fig. 7), which provokes a strong increase of axial velocity, from 1630 m s^{-1} to 4030 m s^{-1} (Fig. 8). Because of this effect the convective term in the energy equation becomes dominant and a strong decrease of temperature, from 13 700 K to 4940 K, is obtained (Fig. 9). As temperatures decrease, the thermal non-equilibrium appears at 2.5 mm from the entry where $T = 10\ 000$ K, and at the exit, a difference of 400 K is obtained ($T = 4940$ K, $T_e = 5340$ K).

The fields of the pressure (Fig. 10), axial velocity (Fig. 11) and heavy species temperature (Fig. 12) are presented for 40 mm exit diameter of divergent nozzle. For this nozzle, the expansion is much stronger than for 20 mm exit diameter, the pressure decreases from 95 kPa to 84 Pa (Fig. 7). The temperatures decrease from 13 700 K to $T = 3180$ K for heavy particles and to $T_e = 4060$ K for electrons (Fig. 9). At the distance more than 5 mm, the radial conductive heat flux is small compared to convective term and the wall condition does not influence the radial variation of the temperature (Fig. 13). A more important deviation from equilibrium condition is observed (Fig. 9). The decrease results in the pressure has for consequence the increase of the velocity (from 1630 m s^{-1} to 4 360 m s^{-1}) which is higher than for the case of nozzle with 20 mm diameter (Fig. 8). In the two divergent cases, the strong variations of plasma jet parameters are observed at the distance of 10 mm from the entry of nozzle due to the expansion effect.

In the core of the plasma jet, where temperature is high (more than 10 000 K), the thermal equilibrium condition is verified, while for lower temperatures (especially near the wall) the thermal non-equilibrium appears.

The degree of ionization α varies only slightly in the nozzle (from 0.27 to 0.25), except near the wall because of the low temperature in that region (close to the wall $\alpha \approx 10^{-3}$). The electron density varies from the inlet of the nozzle 1.3×10^{23} m^{-3} to its exit 4.3×10^{20} m^{-3}.

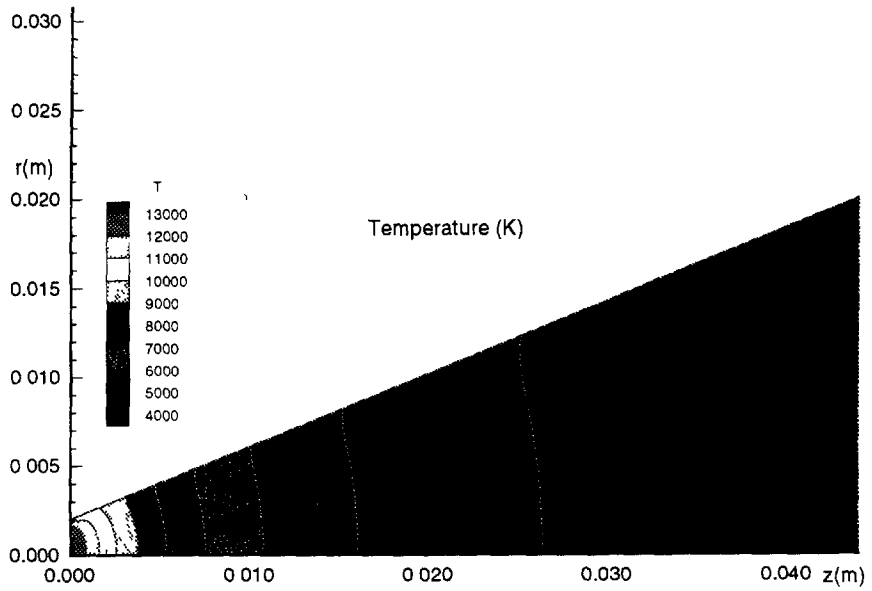

Fig. 12. — Heavy particle temperature field in the divergent nozzle of exit diameter 40 mm.

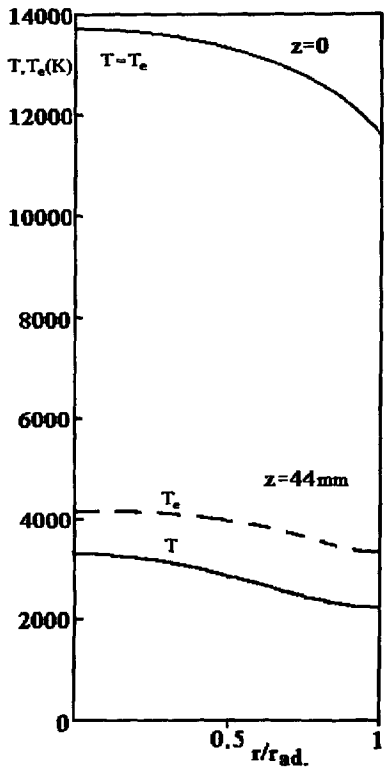

Fig. 13. — Radial distributions of heavy particle and electron temperatures at the inlet and exit of divergent part of the nozzle. The exit diameter is 40 mm.

The radial velocity distribution depends on geometrical shape of the nozzle but its value is negligible compared to the axial velocity ($u/v < 20\%$). If the radial velocity is not taken into account in the resolution of plasma equations, the results obtained show a difference for velocity below 15% and for the temperature below 10%.

For the nozzle 88 mm in length with the same angle than that of the nozzle 44 mm in length and 40 mm in exit diameter, and for the same inlet conditions, at the exit of the nozzle the temperature decreases to 1324 K, the heavy species and electron densities decrease to 7.45×10^{20} m^{-3} and to 2.06×10^{20} m^{-3}, respectively, resulting in an important reduction of the pressure from 95 kPa to 17 Pa, the axial velocity is being only slightly increased (2%).

5. Conclusions

It is well-known that different plasma jets can be obtained changing the operating parameters of plasma torch, however the possibility of obtaining wide variety of plasma jets by this mean is rather limited. The presented calculations show that a wide variety of regimes and properties can be obtained from a geometrical change of the plasma torch nozzle. The results prove that by changing the angle and the length of the nozzle, the plasma jets can be supersonic or subsonic with Mach numbers [6] in the range 0.1–5, as well as in equilibrium or non-equilibrium states. With the geometrical change, the plasma jet can be produced in the range of pressures 100 kPa – 10 Pa, temperatures 16 000–1000 K, electron densities 10^{20}–10^{24} m^{-3}.

Our calculation proves the necessity of optimising the nozzle design, in order to obtain maximal performance of plasma torch and desired values of flow parameters. This numerical code can be used to simulate plasma jets and help in the designing of new plasma torches.

References

[1] Megli T.W., Krier H. and Burton R.L., A Plasmadynamics Model for Nonequilibrium Processes in N_2/H_2 Arcjets, 26th AIAA Plasmadynamics and Lasers Conf., San Diego, AIAA Paper 95-1961 (1995).

[2] Sleziona P.C., Auweter-Kurtz M. and Messerschmid E.W., Numerical Model a Plasma Wind Tunnel Accelerator, 30th AIAA Thermophysics Conf., San Diego, AIAA Paper 95-2110 (1995).

[3] Zheng-Tao Deng, Goang-Shin Liaw and Lynn Chou, Computation of Low-Density Axisymmetric Nozzle Flow Fields by Solving Burnett Equations, 30th AIAA Thermophysics Conf., San Diego, AIAA Paper 95-2008 (1995).

[4] Lelevkin V.M., Kulumbaev E.B., Semenov V.F. and Schram D.C., Modelling of electric arc helium flow inside a profiling channel, ESCAMPIG 96, Poprad, Slovakia, 211 (1996).

[5] Chang C.H. and Pfender E., Nonequilibrium modeling of low-pressure argon plasma jets; Part I: Laminar Flow, *Plasma Chemistry and Plasma Processing* **10** (1990) 473.

[6] Meulenbroeks R.F.G., Engeln R.A.H., Beurskens M.N.A., Paffen R.M.J., van de Sanden M.C.M, van der Mullen J.A.M and Schram D.C., The argon-hydrogen expanding plasma: model and experiments, *Plasma Sources Sci. Technol.* **4** (1995) 74 .

[7] Patankar S.V., Numerical Heat Transfer and Fluid Flow (McGraw-Hill, New York, 1980).

[8] Beulens J.J., Milojevic D., Schram D.C. and Vallinga P.M., A two-dimensional nonequilibrium model of cascaded arc plasma flows, *Phys. Fluids B* **3** (1991) 2548.

[9] Benoy D.A., Modelling of thermal argon plasmas, Ph. D. Thesis, University of Technology (Eindhoven, The Netherlands, 1993).
[10] Hoffert M. and Lien H., Quasi one-dimensional nonequilibrium gas dynamics of partially ionized two temperature argon, *Phys. Fluids* **10** (1967) 1769.
[11] Drawin H.W. and Felenbok P., Data for Plasmas in Local Thermodynamic Equilibrium (Gauthiers-Vilars, Paris, France, 1965).
[12] Hirschfelder J.O., Curtis C. F. and Bird R.B., Molecular theory of gases and liquids (John Wiley & Sons, New York, 1970).
[13] Butler J.N. and Brokav R.S., The thermal conductivity of gas mixtures in chemical equilibrium, *J. Chem. Phys.* **26** (1957) 1636.
[14] Aubreton J. et Fauchais P., Influence des potentiels d'interaction sur les propriétés de transport des plasmas thermiques: exemple d'application le plasma argon hydrogène à la pression atmosphérique, *Revue Phys. Appl.* **18** (1983) 51.
[15] Mitchner M. and Kruger C.H., Partially Ionized Gases (Wiley and Sons, New York, 1973).
[16] Devoto R.S., Transport properties of ionized monoatomic gases, *Phys. Fluids* **9** (1966) 1230.
[17] Kaminska A. et Dudeck M., Rap. du Laboratoire d'Aérothermique, Transferts thermiques dans un arc-jet à basse pression, R. 95-3, CNRS (1995).
[18] Paskonov V.M., Numerical methods of gas dynamic, Pub. Moscow Univ. (1963).
[19] Fletcher C.A.J., Computational Techniques for Fluid Dynamics, vol. 2 (Springer-Verlag, New-York, 1988).